Adaptive Model-Based Predictive Control With Steady State Offset Compensation for a Distributed Solar Collector Field. IEEE-ICNNSP 2003, Dec. 14-17, Nanjing, China

ADAPTIVE NEURAL MODEL-BASED PREDICTIVE CONTROL WITH STEADY STATE OFFSET COMPENSATION FOR A DISTRIBUTED SOLAR COLLECTOR FIELD

P. Gil[†‡] pgil@dei.uc.pt
J. Henriques[†] jh@dei.uc.pt
P. Carvalho[†] carvalho@dei.uc.pt
H. Duarte-Ramos[‡] hdr@fct.unl.pt
A. Dourado[†] dourado@dei.uc.pt

[†]CISUC-Informatics Engineering Department
Universidade de Coimbra, Pólo II 3030 Coimbra
Phone: +351 239790000, Fax: +351 239701266
Portugal

[‡]Electrical Engineering Department, UNL
2825-114 Monte de Caparica
Phone: +351 212948545, Fax: +351 212948532
Portugal

ABSTRACT

An approach to the control of a Distributed Solar Collector field relying on a non-linear adaptive constrained model-based predictive control scheme with steady-state offset compensation is developed and implemented. This methodology is based on a non-linear state-space neural networks within a model-based predictive control framework. The neural network training is carried out online by means of a distribution approximation filter approach. In order to get rid of static offsets an offset compensator is incorporated in the control loop. Tests on the ACUREX field illustrate the feasibility of the proposed approach.

1. INTRODUCTION

For the last few decades model-based predictive control (MPC) methodologies have increasingly been receiving the control community attention and recognition as a valuable approach in solving practical control problems. One example of a successful application of MPC strategy was implemented by the authors in a distributed solar collector field [1].

The MPC history can be traced back to the late 1970's with the Model Algorithm Control and the Dynamic Matrix Control techniques [2], where a linear description of the plant was considered. More recently, pushed by the non-linear nature of most industrial processes, some research efforts have been placed in the development of reliable non-linear model predictive control strategies (NMPC). The main drawback of "true" NMPC approaches is related to the online solution of a non-convex optimisation problem, since the convergence to a feasible/optimal solution and stability cannot be guaranteed in advanced, not to mention the unpredictable computation time that might be required.

Another issue concerning NMPC is that for many systems it might be difficult and rather expensive to come up with an enough accurate physical model of the plant required by MPC techniques. These limitations can mainly be attributed in most cases to the complexity of the underlying phenomena and/or to the lacking of some specific parameters. In these circumstances neural networks have proved to perform quite well in the identification of non-linear systems based on input-output data (see *e.g.* [3], [4] and [5]).

It is well known that neural networks are universal approximators [6], [7]. However, it is also true that the accuracy of the neural predictor is extremely dependent on the quality of the training data set. In case of offline learning, this fact together with a bounded number of iterations and the implementation of regularization techniques in the learning stage inexorably leads to a model/plant mismatch, which is the expression of an impenetrable screen between the world of mathematical description and the real world [8]. Thus, there will be steady state offset errors in the control system response. On the other hand, even in the case where neural network weights are adjusted online this situation might arise as a result of slower adaptation rate compared to the plant's dynamics change. To deal with this effect on the control performance, Draeger *et al.*, [9] suggest adding up to the system's step response an estimate of modelling errors, while the incorporation in the control loop of an offset compensator, only active in a narrow range from the set point, is proposed by the authors [10].

This paper describes the implementation on a Distributed Solar Collector field – Acurex, of a constrained local instantaneous linear model predictive control scheme. The explicit linear model is extracted at each sampling time from the state-space neural network model of the plant trained online. In order to get rid of static offset errors the output are externally fed back such that weighted errors are used to change the reference signals provided to the optimiser.

2. EXTENDED MPC FORMULATION

Model-based predictive control is a discrete-time technique where an explicit dynamic model of the plant is used to predict the system's outputs over a finite prediction horizon P when control actions are manipulated throughout a finite control horizon M [11]. At time step k the optimiser computes on-line the optimal open-loop sequence of control actions such that the predicted outputs follow a pre-specified reference signal and taking into account possible hard and soft constraints. Only the current control actions $u(k\mid k)$ are actually fed to the plant over the time interval $\left[k,k+1\right)$. Next, at time step $k+1$, the prediction and control horizons are shifted ahead by one step and a new optimisation problem is solved using the most recent measurements, and the control action fed to the plant in the previous time interval, $u(k\mid k)$.

Let the linearised discrete-time dynamics of a general non-linear system be described in the state-space form as follows:

$$\begin{aligned} x(k+1) &= \Phi\, x(k) + \Gamma u(k) + \eta \\ y(k) &= \Xi\, x(k) \end{aligned} \tag{1}$$

where $\Phi \in \Re^{n\times n}$, $\Gamma \in \Re^{n\times m}$ and $\Xi \in \Re^{p\times n}$ are, respectively, the state, input and output matrices; $x \in \Re^{n}$ is the state vector, $u \in \Re^{m}$ is the control vector and $y \in \Re^{p}$ the output vector; $\eta \in \Re^{n}$ is a constant vector related to the first term of the Taylor expansion, which is zero at any equilibrium point.

Considering a 2-norm for the cost functional and linear constraints on the inputs and outputs of the system and, additionally, bounds on the rate of change of control actions, the open-loop optimisation problem can be stated in the following way:

$$\begin{aligned} \min_u J = \min_u &\left\{ \sum_{i=1}^{P} \left\| y(k+i\mid k) - r(k+i) \right\|_{Q_i}^2 \right. \\ &\left. + \sum_{i=0}^{P-1} \left\| u(k+i\mid k) \right\|_{R_i}^2 + \sum_{i=0}^{M-1} \left\| \Delta u(k+i\mid k) \right\|_{S_i}^2 \right\} \end{aligned} \tag{2}$$

subject to system dynamics (1) and to the following inequalities:

$$\begin{aligned} &y_{\min} \le y\left(k+i\middle|k\right) \le y_{\max}, \quad i=1,\ldots,\ P, \quad k\ge 0 \\ &u_{\min} \le u\left(k+i\middle|k\right) \le u_{\max}, \quad i=0,\ldots,\ P-1, \quad k\ge 0 \\ &\left|\,\Delta u\left(k+i\middle|k\right)\right| \le \Delta u_{\max}, \quad i=0,\ldots,\ M-1, \quad k\ge 0 \\ &\left|\,\Delta u\left(k+i\middle|k\right)\right| = 0, \quad i=M,\ldots,\ P-1, \quad k\ge 0 \end{aligned} \tag{3}$$

with $Q_i \in \Re^{p\times p}$, $R_i \in \Re^{m\times m}$, $S_i \in \Re^{m\times m}$, $\Delta u \in \Re^{m}$ is the control increment vector and $r \in \Re^{p}$ is the reference signal.

Given the convexity of the optimisation problem any particular solution is a global optimum and thus the open-loop optimal control problem can be restated as a quadratic programming problem:

$$\textit{minimise}\ J\left(\Delta\tilde{u}\right) = h^T \Delta\tilde{u} + \frac{1}{2}\Delta\tilde{u}^T H \Delta\tilde{u} \tag{4}$$

$$\textit{Subject to} \qquad A^T \Delta\tilde{u} \le b \qquad (5)$$

where $A \in \Re^{mM\times(4mM+2pP)}$, $b \in \Re^{(4mM+2pP)}$ and $\Delta\tilde{u} \in \Re^{mM}$ is the extended control increments over the control horizon. The cost function's gradient $h \in \Re^{mM}$ and the Hessian $H \in \Re^{mM\times mM}$ are given by:

$$\begin{aligned} h_l^T = 2&\left\{ x_o^T \left[\sum_{i=l-1}^{P-1} \left(\Xi\Phi^{i+1}\right)^T Q_{i+1} \sum_{q=0}^{i-l+1} \Xi\Phi^q \right]\Gamma - \right. \\ &\left. -\left[\sum_{i=l-1}^{P-1} \left(r(i+1)\right)^T Q_{i+1} \sum_{q=0}^{i-l+1} \Xi\Phi^q \right]\Gamma + u_o^T \sum_{i=l-1}^{P-1} R_i \right\}; \\ &\left\{l=1,\ldots M\right\} \end{aligned} \tag{6}$$

$$\begin{aligned} H_{ll} = 2&\left\{ \Gamma^T \sum_{i=0}^{P-l} \left[\sum_{q=0}^{i} \left(\Xi\Phi^q\right)^T Q_{i+1} \sum_{q=0}^{i} \Xi\Phi^q \right]\Gamma + \right. \\ &\left. + \sum_{i=l-1}^{P-1} R_i + S_{l-1} \right\}; \left\{l=1,\ldots,\ M\right\} \end{aligned} \tag{7}$$

$$\begin{aligned} H_{lp} = 2&\left\{ \Gamma^T \sum_{i=l-1}^{P-1} \left[\sum_{q=0}^{i-l+1} \left(\Xi\Phi^q\right)^T Q_{i+1} \sum_{q=0}^{i-p+1} \Xi\Phi^q \right]\Gamma + \right. \\ &\left. + \sum_{i=l-1}^{P-1} R_i \right\};\ \left\{p=1,\ldots,\ M;\ p\ne l\right\} \end{aligned} \tag{8}$$

In order to prevent from the effect of modelling errors that are responsible for static offsets, an offset compensator is incorporated into the control loop as depicted schematically in Fig. 1.

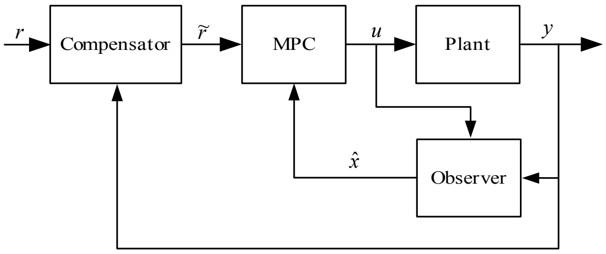

Fig. 1. Extended MPC Structure.

The filter works somehow as an integrator where the control error is previously weighted according to (9). Next, this summation is added up to the true reference signal before being supplied to the MPC structure. Since the weighting factor α is neglectable beyond a narrow range from the set point an effective manipulation of the reference signal provided to the optimizer only takes place in the vicinity of the set point, avoiding this way undesirables windup effects over the reference signal.

$$\alpha(k) = \frac{\kappa}{1+\left[y(k)-r(k)\right]^4} \tag{9}$$

where κ is a user's selected constant.

3. DSC NEURAL MODELLING

The Acurex field modelling is carried out by means of a non-linear state space neural network. This structure comprises 3 layers of neurons, Fig. 2, where the input and the output layers incorporate one neuron, corresponding to the same number of inputs and outputs of the palnt. The number of neurons in the hidden layer was chosen as 2 according to a trade-off between the generalisation performance and the training error. This neural network architecture is of the recurrent type consisting of a feedforward main body where signals are propagate forward from the input neuron to the hidden units and from this layer to the output neuron to produce the network output. Additionally, within the hidden layer are allowed time-delayed (q^{-1}) feedback connections.

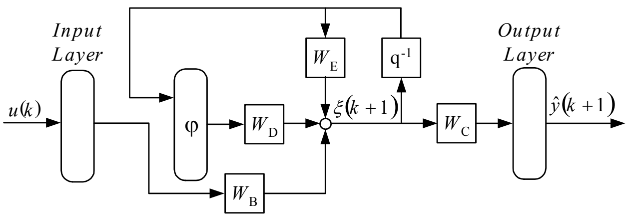

Fig. 2. Non-linear state-space neural network block diagram.

This neural network structure can be described in the state space form by the following equations, assuming φ as a hyperbolic tangent function:

$$\begin{aligned} \xi(k+1) &= W_D \tanh\left(\xi(k)\right) + W_E \xi(k) + W_B u(k) \\ \hat{y}(k) &= W_C \xi(k) \end{aligned} \tag{10}$$

where $\xi(k) \in \Re^{Nn}$ is the network internal hyperstate, $\hat{y}(k) \in \Re^{No}$ is the network output, $u(k) \in \Re^{Ni}$ is the external input; Ni, Nn and No are, respectively, the number of neurons in the input layer, hidden layer and output layer. The synaptic weights between neurons W_B, W_C, W_D and W_E are real-valued matrices with appropriate dimensions.

For the neural network training the present work follows a dual Kalman filter (DUKF) approach based on the unscented transformation [12]. In the DUKF approach both states and weights are computed simultaneously in two stages: *i*) in the time update one step-ahead predictions for the estimates are computed, while *ii*) in the measurement update a correction is provided to these estimates on the basis of current noisy measurement. The dual Kalman filter equations are given by:

Weights estimation

Time update:

$$\Omega(k \mid k-1) = \Omega(k-1 \mid k-1) \tag{11}$$

$$\mathrm{P}_{ww}(k \mid k-1) = \mu^{-1} \quad \mathrm{P}_{ww}(k-1 \mid k-1) \tag{12}$$

$$\mathcal{Z}^w(k \mid k-1) = h\left(\hat{x}(k-1 \mid k-1), \Omega(k \mid k-1), k\right) \tag{13}$$

$$\hat{z}_w(k \mid k-1) = \sum_{i=0}^{2Nw} \Gamma_i^w \mathcal{Z}_i^w(k \mid k-1) \tag{14}$$

$$P_{\nu\nu}^w(k \mid k-1) = \sum_{i=0}^{2Nw} \left\{ \Gamma_i^w \left[\mathcal{Z}_i^w(k \mid k-1) - \hat{z}_w(k \mid k-1) \right] \cdot \left[\mathcal{Z}_i^w(k \mid k-1) - \hat{z}_w(k \mid k-1) \right]^T \right\} + R \tag{15}$$

$$P_{wz_w}(k \mid k-1) = \sum_{i=0}^{2Nw} \left\{ \Gamma_i^w \left[\Omega_i(k \mid k-1) - \hat{w}(k \mid k-1) \right] \cdot \left[\mathcal{Z}_i^w(k \mid k-1) - \hat{z}(k \mid k-1) \right]^T \right\} \tag{16}$$

Measurement update:

$$\mathcal{K}^w(k) = \mathrm{P}_{wz_w}(k \mid k-1) \left(P_{\nu\nu}^w(k \mid k-1) \right)^{-1} \tag{17}$$

$$\hat{w}(k \mid k) = \hat{w}(k \mid k-1) + \mathcal{K}^w(k) \left[z(k) - \hat{z}(k \mid k-1) \right] \tag{18}$$

$$\mathrm{P}_{ww}(k \mid k) = \mathrm{P}_{ww}(k \mid k-1) - \mathcal{K}^w(k) \mathrm{P}_{\nu\nu}^w(k \mid k-1) \mathcal{K}^w(k)^T \tag{19}$$

States estimation

Time update:

$$\mathcal{X}\left(k \mid k-1\right)=f\left(\mathcal{X}\left(k-1 \mid k-1\right),u\left(k-1 \mid k-1\right),\; w\left(k-1 \mid k-1\right),k\right) \tag{20}$$

$$\hat{x}\left(k \mid k-1\right)=\sum_{i=0}^{2Nn}\Gamma_i^x \mathcal{X}_i\left(k \mid k-1\right) \tag{21}$$

$$\mathrm{P}_{xx}\left(k \mid k-1\right)=\sum_{i=0}^{2Nn}\Gamma_i^x\left[\mathcal{X}_i\left(k \mid k-1\right)-\hat{x}\left(k \mid k-1\right)\right]$$

$$\mathcal{Z}^x\left(k \mid k-1\right)=h\left(\mathcal{X}\left(k \mid k-1\right),w\left(k-1 \mid k-1\right),k\right) \tag{22}$$

$$\hat{z}_x\left(k \mid k-1\right)=\sum_{i=0}^{2Nn}\Gamma_i^x \mathcal{Z}_i^x\left(k \mid k-1\right)$$

Measurement update:

$$P_{\nu\nu}^x\left(k \mid k-1\right)=\sum_{i=0}^{2Nn}\left\{\Gamma_i^x\left[\mathcal{Z}_i^x\left(k \mid k-1\right)-\hat{z}_x\left(k \mid k-1\right)\right]\cdot\left[\mathcal{Z}_i^x\left(k \mid k-1\right)-\hat{z}_x\left(k \mid k-1\right)\right]^T\right\}+R \tag{23}$$

$$P_{xz_x}\left(k \mid k-1\right)=\sum_{i=0}^{2Nn}\left\{\Gamma_i^x\left[\mathcal{X}\left(k \mid k-1\right)-\hat{x}\left(k \mid k-1\right)\right]\cdot\left[\mathcal{Z}_i^x\left(k \mid k-1\right)-\hat{z}_x\left(k \mid k-1\right)\right]^T\right\} \tag{24}$$

$$\mathcal{K}^x\left(k\right)=\mathrm{P}_{xz_x}\left(k \mid k-1\right)\left(P_{\nu\nu}^x\left(k \mid k-1\right)\right)^{-1} \tag{25}$$

$$\hat{x}\left(k \mid k\right)=\hat{x}\left(k \mid k-1\right)+\mathcal{K}^x\left(k\right)\left[z\left(k\right)-\hat{z}\left(k \mid k-1\right)\right] \tag{26}$$

$$\mathrm{P}_{xx}\left(k \mid k\right)=\mathrm{P}_{xx}\left(k \mid k-1\right)-\mathcal{K}^x\left(k\right)\mathrm{P}_{\nu\nu}^x\left(k \mid k-1\right)\mathcal{K}^x\left(k\right)^T \tag{27}$$

where μ denotes the forgetting factor, Ω the sigma points matrix of w, Γ the corresponding weight vector, $\mathcal{K}$ the Kalman gain and $\mathcal{X}$ the sigma points matrix of x.

4. THE SOLAR THERMAL POWER PLANT

The ACUREX distributed solar collector field (DSC) is part of the Plataforma Solar de Almería (PSA), Fig. 3. It is a center for testing thermal solar energy applications, located on the desert of Tabernas, in the South of Spain.

Fig. 3. The distributed solar collector field at PSA

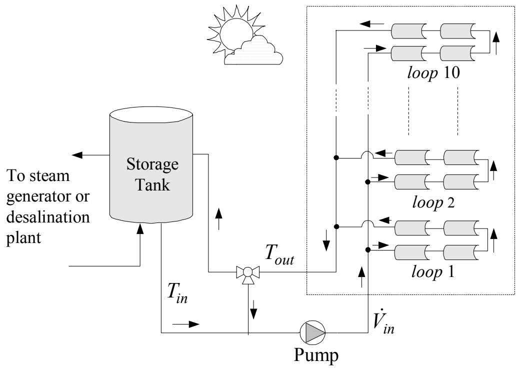

Fig. 4. Distributed solar collector field schematics.

The DSC field consists of 480 parabolic trough collectors arranged in 20 rows aligned on a West-East axis and forming 10 independent loops as depicted in figure 4. Every solar collector has a linear parabolic-shaped reflector that focuses the sun's beam radiation on a linear absorber tube located at the focus of the parabola. Each of the loops is 172 *m* long, with an active section of 142 *m*, while the reflective area of the mirrors is around 264.4 m^2.

The heat transfer fluid used to transport the thermal energy is the Santotherm 55, which is a synthetic oil with a maximum film temperature of 318 °*C* and an autoignition temperature of 357°*C*. The thermal oil is heated as it circulates through the absorber tube before entering the top of the storage tank. The colder inlet oil is extracted form the bottom of the tank. A three way valve located at the field outlet enables the oil recycling (by-passing the storage tank) until its outlet temperature is high enough to be sent to the storage tank. The thermal energy storage in the tank can be subsequently used to produce electrical energy in a conventional steam turbine/generator or in the solar desalination plant operation.

The DSC field is provided as well with a sun tracking system, which causes the solar collector to revolve around an axis parallel to the receiver in order to follow the yearly variation of the sun's declination.

5. ACUREX FIELD TESTS

The main control prerequisite in a DSC field is to maintain the outlet oil temperature at a prescribed value by suitably manipulating the oil flow rate through the receivers. For this purpose, the proposed adaptive constrained non-linear MPC scheme with steady state offset compensation was tested on the Plataforma Solar de Almería Acurex field in July 2002.

In all tests reported in this paper the sampling time was set to 15 seconds and the prediction horizon and the control horizon were chosen as $P=10$ and $M=1$ time steps. Further, cost functional weight matrices were chosen as:

$$Q_i = \begin{cases} 5 \ , \ i = 1,\ldots,P-1 \\ 100 \ , \ i = P \end{cases} \quad \mathcal{R}_i = 10^{-3} \ , \ i = 0,\ldots,P-1 \quad S_i = 10^{-4} \ , \ i = 0,\ldots,M-1 \tag{28}$$

For safety reasons, constraints were imposed on the oil flow rate, which should be within 2 ls^{-1} and 10 ls^{-1} and on the outlet oil temperature which is limited to 300°C. Additionally, the oil flow rate moves were constrained to 0.1 ls^{-1} in order to enable a smoother pump operation.

A. *Test on 17th July: Adaptive MPC*

In this test an adaptive neural model-based predictive control without steady offset compensation was used for controlling the DSC field.

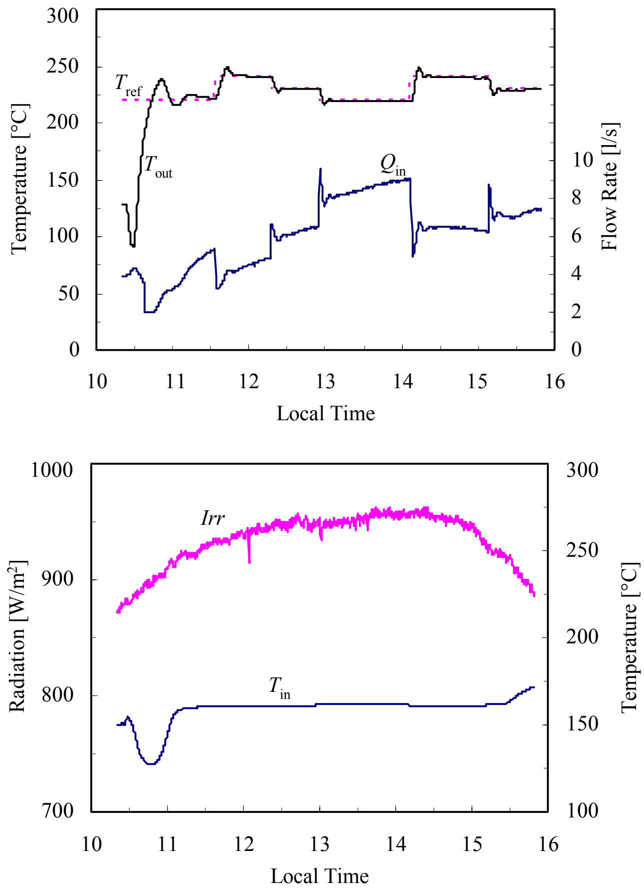

Fig. 5. ACUREX field test on the 17th July: Set point, outlet oil temperature and oil flow rate, solar radiation and inlet oil temperature

The main goal with this experiment was to gather information upon the performance of the control system without any offset compensation and to get a reliable term of comparison so as to enable assessing the performance of the steady-state offset compensation approach. The initial covariance matrices involved in the weights adaptation computations were chosen as $P_{xx}(0) = \mathbf{1}$ and $P_{ww}(0) = diag(5\times10^{-3})$ and the forgetting factor μ was set equal to 0.9986.

In figure 3 it is shown the outlet oil temperature (T_{out}), set point (T_{ref}), oil flow rate through each DSC loop (Q_{in}), the inlet oil temperature (T_{in}) and the solar radiation (Irr). As can be observed from the above plots, the adaptive MP control system provides upon the whole a very acceptable response of the outlet oil temperature. Furthermore, as time goes on, as a result of an increasing model accuracy the steady state errors become gradually lower. However, in view of the fact the adaptation mechanism is rather smooth when the solar radiation starts falling after the noon the neural predictor becomes less accurate and so offset errors are once again observed. This new dynamics would be captured in case the test had not been stopped.

B. *Test on 23rd July: Adaptive MPC plus Offset Compensation*

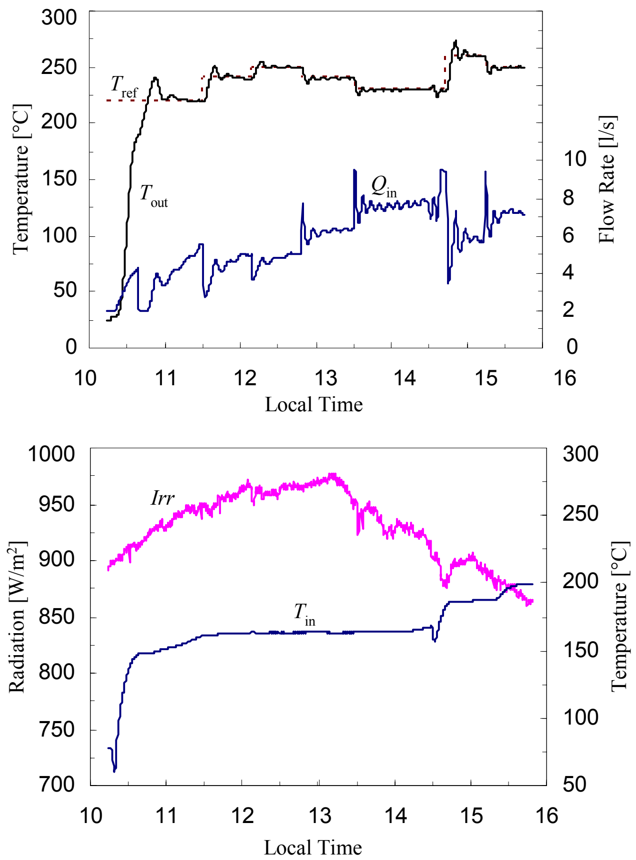

Fig. 6. ACUREX field test on the 23th July: Set point, outlet oil temperature and oil flow rate, solar radiation and inlet oil temperature.

This control test was carried out using an adaptive neural model-based predictive control incorporating a steady offset compensator. The initial covariance matrices for the DUKF were chosen as $P_{xx}(0) = \mathbf{1}$ and $P_{ww}(0) = diag(2 \times 10^{-3})$. Further, the forgetting factor was set equal to 0.9987 and $\kappa = 0.005$.

Figure 4 shows the outlet oil temperature (T_{out}), set point (T_{ref}), oil flow rate through each DSC loop (Q_{in}), the inlet oil temperature (T_{in}) and the solar radiation (Irr). As can be observed from the above plots, this MPC scheme is able to drive the outlet oil temperature to the desired value even in the initial control stage where it is expected significant modelling errors. However, the price to pay is a more oscillating control system time response.

6. CONCLUSIONS

In this paper an adaptive constrained model-based predictive control scheme with steady state offset compensation is applied to the distributed collector field of a solar power plant at the Plataforma Solar de Almería. This strategy was compared with an adaptive MPC strategy without incorporating an offset compensator so as to assess the proposed control system performance. Experimental results show the feasibility of the proposed control scheme and suggest further studies in order to improve its performance.

ACKNOWLEDGEMENTS

This work was partially supported by POSI– *Programa Operacional da Sociedade de Informação* of Portuguese Fundação para a Ciência e Tecnologia and by the European Union's FEDER and PRAXIS XXI ALCINE Projects. The experiments were carried under the support of the "Improving Human Potential" programme of EU-DGXII. The authors wish to express their gratitude to the PSA staff.

REFERENCES

[1] Gil, P., J. Henriques, P. Carvalho, H. Duarte-Ramos and A. Dourado, "Adaptive Neural Model-Based Predictive Control of a Solar Power Plant," *IEEE International Joint Conference on Neural Networks*, Honolulu, HI-USA, 2002.

[2] Garcia, C., D. Prett and M. Morari, "Model predictive control: Theory and practice – a survey," *Automatica*, vol. 25, 3, pp. 335-348, 1989.

[3] Rivals, I., and L. Personnaz, "Black-box modelling with state-space networks," *Neural Adaptive Control Technology, R. Zbikowski and J. Hunt eds., World Scientific*, pp. 237-264, 1996.

[4] Yamada, T., and T. Yabuta, "Dynamic System Identification Using Neural Networks," *IEEE Trans. On Systems, Man and Cybernetics*, Vol. 23, No.1, pp. 204-211, 1993

[5] Narendra, K., and K. Parthasarathy, "Identification and Control of Dynamical Systems Using Neural Networks," *IEEE Trans. On Neural Networks*, Vol. 1, No. 1, pp. 4-27, 1990.

[6] Funahashi, K., "On the approximate realization of continuous mappings by neural networks". *Neural Networks*, vol. 2, pp. 183-192, 1989.

[7] Hornik, K., M. Stinchcombe and H. White, "Multilayer Feedforward Networks are Universal Approximators," *Neural Networks*, vol.2, pp. 359-366, 1989.

[8] Ljung, L., "System Identification: Theory for the User," Prentice-Hall, Inc., Englewood Cliffs, New Jersey, 1987.

[9] Draeger, A., S. Engell and H. Ranke, "Model predictive control using neural networks," *IEEE Control Systems Magazine*," vol. 15, no. 5, pp. 61-66, 1995.

[10] Gil, P., J. Henriques, A. Dourado and H. Duarte-Ramos, "Constrained Neural Model Predictive Control with Guaranteed Free Offset," *Proc. 2000 IEEE Int. Conf. on Industrial Electronics, Control and Implementation – IEECON*, Nagoya, Japan, pp. 1991-1996, 2000.

[11] Maciejowski, J., "Predictive Control with Constraints," Prentice Hall, 2002.

[12] Julier, S., J. Uhlmann and F. Durrant-Whyte, "A New Method for the Nonlinear Transformation of Means and Covariances in Filters and Estimators," *IEEE Trans. Aut. Control*, vol. 45, pp. 477-482, 2000.